Experimental Characterization of a Radio Frequency Microthermal Thruster

Shae Williams
Purdue University
701 W. Stadium Ave. West Lafayette, IN 47907; (765)838-2253
sewillia@purdue.edu

Ivana Hrbud
Purdue University
701 W. Stadium Ave. West Lafayette, IN 47907
ihrbud@purdue.edu

ABSTRACT

In this paper, the results of the first experimental tests on an RF (Radio Frequency) microthermal propulsion system are reported. A brief synopsis of existing propulsion systems for the 10-100 micronewton thrust regime suitable for microsatellites is presented, with cold gas thrusters the currently dominant option due to their reliability, low weight and volume requirements, and lack of complexity. RF microthermal thrusters are also low-requirement compared to most candidate propulsion subsystems, operate on well-understood theoretical principles, and in testing with argon have demonstrated specific impulses as high as 80-85 seconds with a suboptimal propellant and geometry, implying a higher ultimate performance is attainable. Performance is shown to depend linearly on power input, but that performance improves significantly at lower mass flow rates around 0.1 mg/s. Further, the frequency of the RF voltage applied across the coaxial electrodes has a large and nonlinear effect on performance. These trends will both be studied further in later research.

INTRODUCTION

RF microthermal thrusters have the potential to be a competitive technology for microsatellite applications- delivering two to three times higher specific impulse at equal thrust levels than a cold gas thruster. This approaches the specific impulse available from other non-electric micropropulsion technologies while avoiding many of the pitfalls that make using those technologies problematic in a microsatellite application. RF microthermal thrusters don't require much power, on the order of 10-20 watts. They require little voltage, able to draw directly from a typical spacecraft bus at ~100 V. They have a simple and potentially small optimized geometry, as in the configuration studied for this research they are a pair of coaxial electrodes of which one is grounded and one has an oscillating voltage applied. Further, they are in terms of controllability and storage equivalent to a cold gas thruster, without exotic or reactive propellants required. Because of all these factors, if the performance of RF microthermal satellites shows sufficient improvement over cold gas, for some missions they show promise of being competitive for selection as propulsion aboard a microsatellite.

Microsatellites, typically defined as satellites between 10 and 100 kilograms, have been identified as a key future market for the satellite industry[1] due to their low cost and flexibility. Unfortunately, a major technical challenge of satellites at this mass range has been how to design a propulsion system that is of sufficiently low mass to fit on board, requires sufficiently low power and volume to function, can last sufficiently long to carry out a multi-year mission, and can provide a strong enough performance to actually aid the mission. This has not been a trivial task. To date, most commercial microsatellites have used commercially available cold gas thrusters, with specific impulses in the region of 50 to 70 seconds[2]. This is relatively poor performance which necessitates either the carrying of prohibitive amounts of propellant or demands that mission lifetime be abbreviated and the thruster requirements curtailed- the cited cold gas thruster can deliver a lifetime total impulse of only 380 Newton-seconds. Cold gas thrusters are, however, exceptionally lightweight and not power intensive- still, with more efficient propulsion microsatellite missions could be greatly extended, and new missions could be made feasible. The focus of this research is around the 10-100 micronewton thrust regime, where such small satellites could use thrusters for orbital maintenance and small orbital adjustments.

Existing technologies run into problems when attempting to deliver a system appropriate to this class of satellite. Chemical propulsion is one broad option.

Bipropellant thrusters are not generally feasible- they suffer precision in mass flow control losses that are prohibitive at the micronewton scale, and the tankage and plumbing systems required rapidly overwhelm the mass and space available. Monopropellant thrusters with a catalyst, then, are a better choice- but these too have problems, as the thrust/weight ratio of chemical propulsion declines quickly as scale is reduced to the micronewton range.[3] A catalyst-driven hydrogen peroxide thruster capable of 150-180 seconds specific impulse at thrust ranges in the hundreds of micronewtons is being studied in Austria, but has not yet been able to be fired in vacuum conditions and in any case suffers the drawbacks of requiring a catalyst bed, somewhat hazardous material handling, has to worry about contamination of exposed surfaces on the microsatellite, and so on. Still, the performance of this thruster makes a good ultimate target for the RF microthermal thruster, as it aims at similar mission profiles.

With chemical propulsion presenting such problems, electrical propulsion is a widely studied field for microsatellite propulsion. Only propulsion options relevant to the range of study for this thruster in the regime of tens to hundreds of micronewtons, are studied- in the entire 'microthruster' range, which spans from nanonewtons to tens of millinewtons, a huge number of concepts are under investigation. Only some will be specifically mentioned here. Laser-ablation thrusters, which work by shining a laser onto a volatile solid fuel and vaporizing it, are viable candidates for the low end of the thrust range an RF microthermal thruster would cover, the tens of micronewtons thrust range. However, published results show[4] that at contemporary thrust-to-power ratios, a microthruster that wanted to develop 100 micronewtons of thrust would require on the order of 500 W, which is a prohibitive amount of power for a 10-100 kg microsatellite to devote to propulsion. Tens of micronewtons and tens of watts, however, are feasible- and with a specific impulse of up to 300 seconds and an extremely small minimum impulse bit, desirable if more thrust is not a requirement. Others, like a micro-pulsed plasma thruster (microPPT) under development by the Air Force[5], are more explicitly focused higher than the RF microthermal thruster's design range of 100-1000 micronewtons, and deliver very good specific impulse performance of up to 200 seconds with low power requirements. They suffer, however, from a higher minimum impulse bit than many other options, and power conditioning is a concern. Most electromagnetic devices such as the ones above, however, are still targeted at thrust ranges in the 1-10 micronewton regime for extremely high precision applications like space interferometer attitude control. Additionally, a major problem with many such applications are that microsatellite buses tend to operate at low voltages, at or under 100 V; most electric propulsion devices demand significantly higher voltages, as is the case with the more familiar ion thrusters or MPD thrusters. The RF microthermal thruster can operate well under 100 V, making the required power conditioning equipment much smaller.[6]

More electrothermal-based thruster options are also under consideration for this flight range. These, however, suffer the opposite problem as the electromagnetic thrusters studied- they are optimized more usually for the millinewton thrust regime, which for a microsatellite can be overkill. This applies to both the arcjet and resistojet types of electrothermal device- however, a much more comparable device exists, that of the microwave (as opposed to RF) electrothermal thruster. These deliver specific impulses of over 300 seconds, however are also optimized for use at high power and higher voltages due to their much higher frequencies, on the order of kilowatts instead of the tens of watts an RF microthruster can function on.[7] For this reason, currently studied electrothermal thrusters are not suited for use in microsatellite applications.

The RF microthermal thruster, then, can fill a niche in microsatellite propulsion that is currently underserved, that of missions where thrust requirements vary from the low teens to the low hundreds of micronewtons of thrust. Similar minimum impulse bits to cold gas thrusters can be obtained by identical valving as a cold gas thruster, making them suitable at low thrust levels for attitude control and at high thrust levels for orbit determination. Unusual among electric propulsion devices, they require both low power (<100 W) and low voltages (<100 V), and can operate on an inert propellant- in this research, argon, although other propellants with a potentially higher performance will be studied later. This greatly simplifies the problem of getting these thrusters to work well inside the stringent requirements of microsatellites. The only remaining problem left is their potentially low performance. However, experimental results presented here show that even with an unoptimized thruster geometry in a very narrow design space, specific impulse can be increased by 80-85% over an identical thruster and identical propellant operating as a cold gas thruster. Further improvements in performance, then, seem likely with a more careful thruster design and more comprehensive design space analysis. This would make RF microthermal thrusters an extremely attractive option for microsatellite propulsion.

Despite the possibilities, RF microthermal thrusters have not been heavily studied. To date, the only

research into this specific type of thruster has been analytical modeling performed by William Stein cited above at Purdue for his doctoral research, and preliminary low vacuum tests focusing on electrode erosion. No significant performance-based testing of this type of thruster has been performed. RF thrusters have instead historically been studied in an electromagnetic mode, where the thrust derives from the interaction of electromagnetic fields with charged particles[8]. These have some of the above problems of requiring kilovolts of potential even at low wattage, making their usability for microsatellites dubious. To use this high frequency, low power combination to heat a working fluid seems counterintuitive due to the apparent massive losses to be suffered in heating the thruster as well as the inevitably lower performance ceiling of working in a thermal instead of electromagnetic paradigm. However, as has been shown, there is a niche for such a thruster- and as will be shown, the performance of that type of thruster is extremely promising.

THEORETICAL BACKGROUND AND ANALYSIS

The RF microthermal thruster functions by using a capacitively coupled discharge between a pair of coaxial electrodes to weakly ionize and heat a flow of argon. Once heated, the argon plasma is exhausted through a narrow orifice to thermodynamically convert the plasma's heat into kinetic energy in the same way a conventional rocket engine does. In this way, the RF microthermal thruster can be considered analogous to an arcjet, whose 'arc' is diffuse and covers the entire thruster chamber, driven by an alternating current instead of a direct current. The primary benefit of using an RF discharge instead of a DC arcjet for propellant heating is that, due to the physics of the plasma inside the thruster, high-energy particles are kept away from the electrode walls; this decreases the erosion of electrodes, or sputtering, and thus increases system lifetime.

For simplified modeling purposes, consider the thruster to be infinite parallel plates with a plasma in the middle. A time-varying voltage is placed across the two plates with peak amplitude V_{rf} and frequency ω. Plasmas are joined to physical surfaces by thin positively charged layers called sheaths that arise due to the electrons in the plasma having significantly greater velocity than ions, due to their higher charge-to-mass ratio. Figure 1 shows an illustration of what these sheaths look like between parallel plates. The figure on the left shows a thin sheath (the boundary represented by a dashed line) insulating the neutral bulk plasma from the walls; the two lines represent the number density of positive ions (solid) and negative electrons (dashed). This structure in turn forms a potential shape between the two electrodes that is illustrated on the right of Figure 1. The maximum potential inside the bulk plasma is the plasma potential; it drops sharply to 0 at each electrode. This sets up an electric field that is zero inside the bulk plasma, but strongly points towards the electrodes on either side, which acts as a well trapping electrons inside the bulk plasma and a hill pushing ions toward each wall.

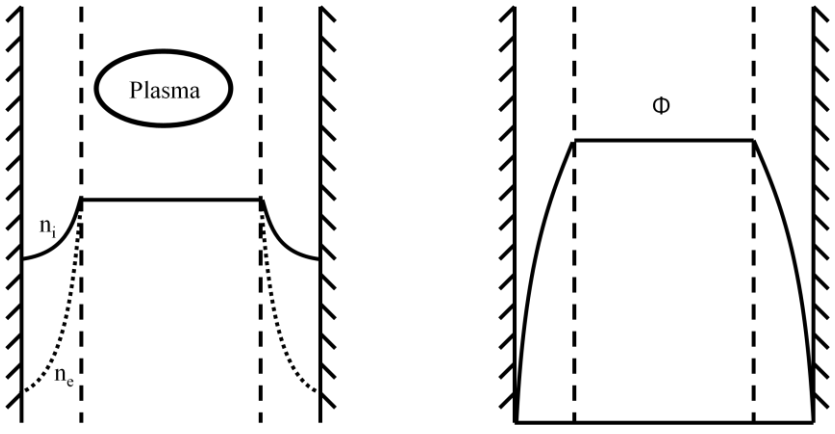

Figure 1: Plasma sheath schematic: on the left, the ion and electron densities between two electrodes, and on the right the potential 'well' formed by the sheaths

If the driving voltage is time-variant instead of constant, the most important effect is that the sheath boundaries- the dashed lines in the figure above- oscillate back and forth with a frequency equal to that of the driving voltage. Other effects also occur, but are not considered for this simplified model. To make the math easier without qualitatively altering the physics, a number of assumptions were made. Ions respond only to time averaged potentials, since they are so heavy; electrons, however, respond to the instantaneous potentials. This is for our regime on the order of 100 MHz a reasonable assumption. We also assume, contrary to the figure above, that the electron density inside the sheaths is 0 and that the ion density is constant between the electrodes. This is akin to assuming that no ion-neutral collisions occur in the sheaths. With these assumptions, equations simplify greatly for a preliminary analysis. The goal of using an RF discharge is to heat the plasma between the electrodes- attention, then, focused on the heating mechanisms at play inside the plasma. Two such mechanisms are important; ohmic, or bulk heating and stochastic heating.

Ohmic heating arises because the plasma has an impedance; putting a time varying voltage across the plasma causes a current to flow through the plasma, which in turn causes a power loss equivalent to the voltage across the plasma times the current passing through the plasma. Rearranging terms and using the more convenient conductivity instead of resistivity, we find the following expression for average power absorbed by ohmic heating of the plasma per unit area:

$$\bar{S}_{ohmic} = \frac{J_1^2}{2} * \frac{d}{\sigma} \quad (1)$$

J_1 is the current density passing through the plasma in amps per square meter, d is the distance between electrodes and σ is the plasma conductivity. This can be restated in more convenient variables as:

$$\bar{S}_{ohmic} = \frac{J_1^2}{2} * \frac{m\nu_m d}{ne^2} \quad (2)$$

Here, ν_m is the electron-neutral collision frequency, m is the electron mass, n is the number density of neutral atoms, and e is the fundamental charge of an electron.

Stochastic heating is a consequence of the phenomenon, noted above, where the sheath boundary oscillates back and forth at the frequency of the driving voltage. Even while oscillating, these sheath boundaries still act to push electrons away from the electrodes in elastic collisions. Because the wall has its own externally driven velocity, this adds energy to the electrons, causing the flow to heat up. Using elastic collisions as a model, the net increase in energy per electron collision with the sheath boundary is

$$dE = 2m * ({u_{es}}^2 - u u_{es}) \quad (3)$$

In this equation, u is the velocity of the electron before impacting the sheath parallel to the sheath, and u_{es} is the velocity of the electron sheath. Since the first of those is a distribution, assumed to be Maxwellian, and the second is a time-varying sinusoid, calculating the power transfer per unit area is not straightforward. Integrating across all incident velocities and averaging over time removes the frequency term, the average power absorbed by stochastic heating of the plasma per unit area can be written as:

$$\bar{S}_{stoch} = \frac{J_1^2}{2} * \frac{m\bar{v}_e}{ne^2} \quad (4)$$

This is similar to the equation for ohmic heating, with the only change being to replace the electron-neutral collision frequency and the size of the gap between electrodes with the average velocity of an electron in the plasma. The combined average power absorbed in heating the plasma per unit area then can be written, considering that stochastic heating occurs on both sheaths and if we neglect for now the power lost by ion collisions with the wall:

$$\bar{S}_{total} = \frac{J_1^2}{2} * \frac{m*(2\bar{v}_e + \nu_m d)}{ne^2} \quad (5)$$

Calculating this numerically requires knowledge of the current density in the plasma. This is not a parameter measured in the lab- instead, frequency and the voltage applied to the plasma are the parameters physically measured. Restating the above equations in these terms, after many ancillary equations and computations we find that

$$\bar{S}_{ohmic} = 1.73 * \frac{m}{2e} * \frac{n_s}{n_o} * \epsilon_0 \omega^2 \nu_m {T_e}^{1/2} {V_1}^{1/2} d \quad (6)$$

$$\bar{S}_{stoch} = 0.45 * \left(\frac{m}{e}\right)^{1/2} * \epsilon_0 \omega^2 \nu_m {T_e}^{1/2} V_1 \quad (7)$$

The full derivation is omitted for space and clarity. Above, the ratio n_s/n_0 is the ratio of ion number densities in the sheath and in the bulk plasma, while T_e and V_1 are the bulk plasma electron temperatures and the voltage drop across the plasma respectively. Given inputs of thruster geometry, incoming propellant pressure and temperature, and the RF voltage amplitude and frequency the simplified

model becomes a system of equations with a single solution for electron temperature and power absorbed. Once the power absorbed into the plasma is known, we can estimate how much heating occurs in the flow quickly by calculating,

$$\Delta T = \frac{A_{electrode} * (S_{ohmic} + 2S_{stoch})}{\dot{m} c_p} \quad (8)$$

With the final temperature of the propellant known, the specific impulse can be quickly calculated from thermodynamics. For argon, the specific impulse of a thruster exhausting at sonic velocity through an orifice heated to T_{final} can be calculated:

$$I_{sp} = 2.633\sqrt{T_{final}} \quad (9)$$

Thus, for a cold gas thruster using argon at ~300 K, the specific impulse would be approximately 46 seconds, and if the argon is heated to ~1500 K the specific impulse improves to approximately 105 seconds. This calculation assumes that insufficient ionization occurs to significantly alter the gas parameters such as specific heat in the plasma. Argon is the propellant used so far in testing this thruster, due to availability and ease of use. Nitrogen and lighter noble gases such as helium or neon would theoretically give superior performance, and additional gases will be tested in the future.

The above highly simplistic analysis gives several useful pieces of information. The first hints at scaling laws. Both types of heating scale with the square of the frequency of the driving voltage. This intuitively makes sense- the higher the frequency, the more rapidly charged particles inside the plasma will be accelerated back and forth. The power absorbed also scales with the amplitude of the applied voltage, but not by a common amount. This too makes intuitive sense; the stronger the applied voltage, the steeper the electric fields and again the faster the charged particles will oscillate. This change in exponent of the dependence of heating on applied voltage causes an interesting phenomenon- at some regimes in the testing program, ohmic heating should dominate, while at others stochastic heating should dominate. In general, the lower the pressure, the more significant stochastic heating becomes; this is relevant since the controlling parameter of pressure inside the thruster is the mass flow rate of propellant, with ramifications that will be shown in the results section.

Simplifying the model to this extent also allowed a computer model of the thruster's performance to be coded that could run extremely rapidly to provide at least a sense of what trends and rough magnitudes of specific impulse the thruster should develop at different conditions. The model was coded, and run over the following parameter space enumerated in Table 1:

Table 1: Parameter Space for Theoretical Run

Parameter	Value	Units
Mass flow	0.1-0.5	mg/s
Power	10-50	W
Frequency	100-200	MHz

This overlapped with the experimental tests already performed. The runs were plotted, and important figures are shown below. The first, Figure 2, shows the specific impulse resulting from the theoretical model with an argon mass flow of a tenth of a milligram per second, across the power and frequency spaces chosen. As expected from just looking at the equations, specific impulse (which is proportional to the square root of heating) scales linearly with frequency and with approximately the square root of power applied. As a note, in the model, the RF voltage is derived from the forward power and a knowledge of how much power is reflected from an impedance mismatch with the thruster that will be addressed in the future. The model also predicts extremely large amounts of heating at this low mass flow rate, up to a maximum of nearly 4000 K at the highest power and frequency calculated. This is unrealistic- heat transfer to the walls among other losses will degrade this performance significantly, as will be shown in the experimental results to date.

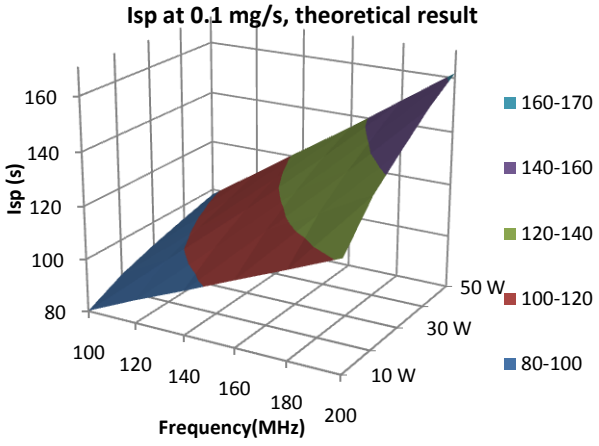

Figure 2: A Section of the Theoretical Performance Results for the RF Microthermal Thruster

Variation of performance with changing mass flow rates, however, is not explicitly in the equations presented above. Figure 3 shows a section of the results holding the power constant at 20 watts, varying frequency and mass flow rate. There is a very clear and large increase in specific impulse at lower mass flow rates, on the order of a 50% increase from dropping mass flow rate from 0.5 to 0.1 milligrams per second. This arises because while increasing the pressure inside the thruster does help the plasma absorb power, it does not do so to enough of a degree to compensate for the additional mass that requires heating. As a result, increasing the pressure (and mass flow rate) decreases the final temperature of the plasma and hence decreases the performance of the thruster. This suggests that the best use of the RF microthermal thruster should be in lower-thrust applications where approximately 100 micronewtons is desirable. This prediction, of improved performance at lower mass flow rates, was confirmed by the preliminary testing, although it was not quite as dramatic a difference as theory predicted.

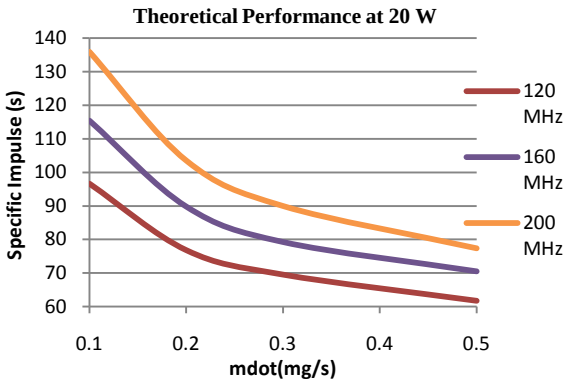

Figure 3: Constant-Power Section of Theoretical Results

With a basic theoretical model complete, and with an idea of the dominant controlling factors governing thruster performance, testing results could be used as an order-of-magnitude check and verification for the model and vice versa. The theoretical results moreover strongly imply that the goal laid out in the previous section, RF microthermal thrusters that could compete on an efficiency basis with monopropellant thrusters, is achievable due to the high predicted specific impulses.

EXPERIMENTAL SETUP

Vacuum Chamber

All research for this dissertation is performed at the Laboratory of Electrical and Advanced Propulsion (LEAP) at Purdue University. There are three parts to the experimental setup- the vacuum system itself that creates the conditions necessary for tests, the thrust stand and associated instrumentation that records data from the tests, and the data acquisition and software that renders that data into a usable form. The vacuum chamber itself is an approximately 4 feet across by 8 feet long cylinder with pumps capable of driving the chamber to an ultimate pressure around 1 microtorr. The propellant delivery system is a custom panel built around a mass flow controller that can deliver up to 2.2 mg/s of a gas, in this case argon, with high accuracy. In practice, however, testing is limited to roughly half that value due to the inability of our vacuum system to maintain low pressures at very high mass flow rates.

The thrust stand which does the measuring of our performance is shown in picture form in Figure 4 and schematically in Figure 5. It is a torsional thrust stand, where the thruster being tested produces a force in one direction torquing the entire three foot long moment arm around a center bulkhead, held by torsional springs with a known spring constant and producing a deflection at the other side measured by a Linear Variable Differential Transformer (LVDT) which measures displacements with sub-micrometer accuracy. There is an oil-bath damper near the thruster, which acts to cut down the duration of moment arm oscillation when a force is applied. Electrostatic fins are attached at the same distance from the bulkhead as the thruster, and serve as part of the calibration procedure. The function of these fins will be addressed further in the next section of this paper.

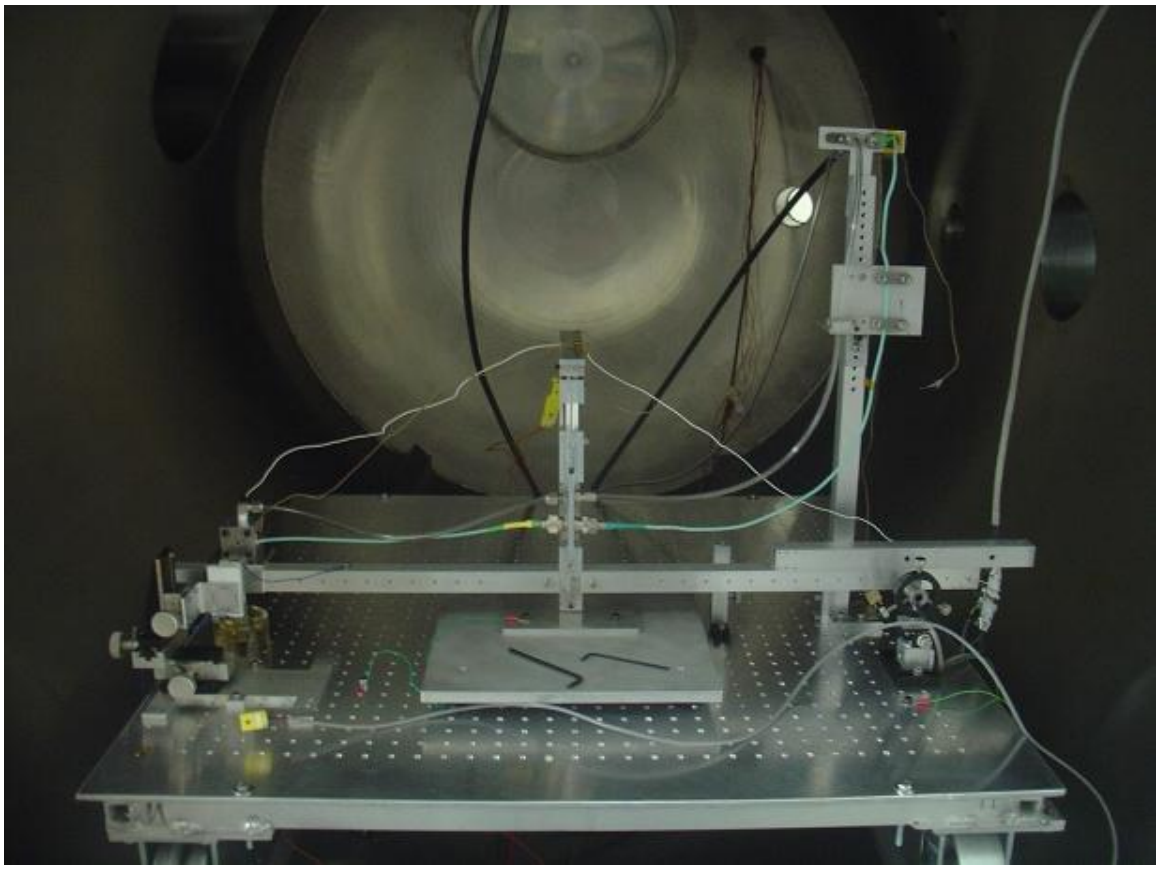

Figure 4: Picture of the Micronewton Thrust Stand

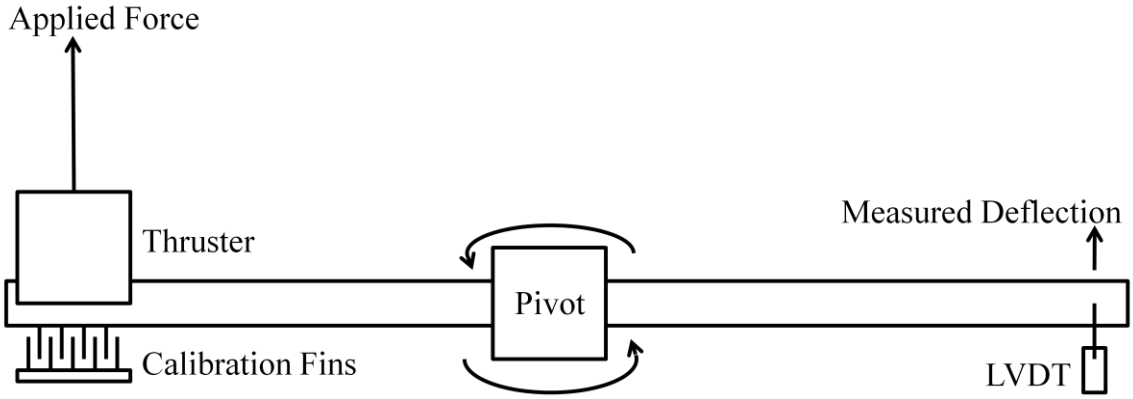

Figure 5: Schematic of the Micronewton Thrust Stand.

Thruster Hardware

The thruster attached to the thrust stand in Figure 4 is an old generation of thruster, and the one all the data in this report has been gathered with- since these results were gathered, a similar new thruster has been machined although there is not yet sufficient data with the new hardware to present. Figure 6 and Figure 7 show a picture and a schematic of this thruster. A nozzle plate is shown beside the thruster in Figure 6, and attached (and electrically connected to the outer electrode) in Figure 7. The thruster in its simplest form consists of a pair of coaxial electrodes between which gas flows and is excited by an RF voltage. The inner, cylindrical electrode rests in a ceramic dielectric holder for structural support and to

keep the impedance of the thruster around 50 ohms until the point where propellant begins to flow. An electrical connection to the RF power supply is made through the side of the thruster, screwing into the inner electrode- the outer electrode is the entire metal body of the thruster, and is connected to ground through the vacuum chamber itself. Argon gas flows through the port in the top of the thruster, spends some time in the energetic RF field between the electrodes, heats up and partially ionizes, then streams out through a nozzle plate, generating thrust via thermodynamic expansion. This design will be altered later in research as more knowledge of the design space is available.

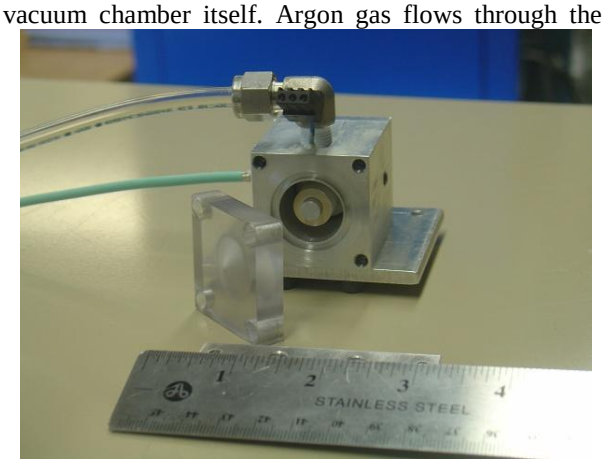

Figure 6: Picture of RF Microthermal Thruster. A Nozzle Plate and Ruler are Shown for Scale

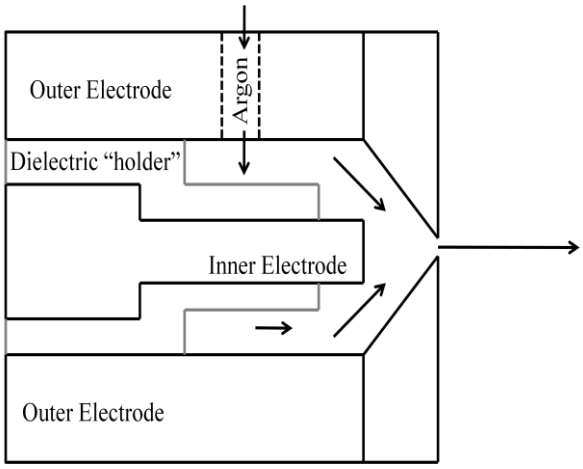

Figure 7: Schematic of the Thruster with a Nozzle Plate On

COMPLETED WORK

Calibration

Great care was taken to ensure the reliability and repeatability of thrust measurements on the order of 10 to 1,000 micronewtons with a target resolution of +/- 1 micronewton. To be able to deliver a repeatable and extremely well known force in vacuum is not itself a trivial task, but was the starting point of being able to calibrate the torsional thrust stand. Prior work at LEAP developed an electrostatic fin system capable of delivering a sufficiently repeatable micronewton scale force at any conditions from atmosphere to high vacuum.[9] The electrostatic fin system places a voltage differential of up to 1 kilovolt on a pair of sets of aluminum fins that interlace like the blades of a zipper without touching. For a range of fin separations from ~0.4-0.6 mm, doing so produces a force between 0 and 810 micronewtons that is repeatable with an error of under a micronewton in either direction. Additionally, it is a noncontact force, so the inertia of the thrust stand isn't altered. This system was chosen to be the basis of all calibrations for this research. To perform a calibration run, the voltage differential across the fins is steadily increased from 0 to 1000 V, pausing at each step to let the oil damper cancel out transient oscillations; once acceptably settled, the voltage reading of the LVDT is taken and the voltage is increased again. To check for hysteresis, once 1000 V is reached more data is taken at the same or similar voltage readings on the way back to 0. Hysteresis is usually not a factor, at or below the micrometer level on the LVDT. Shown below, in Figure 8, is a typical recent calibration result translated from raw voltages into micronewtons and micrometers.

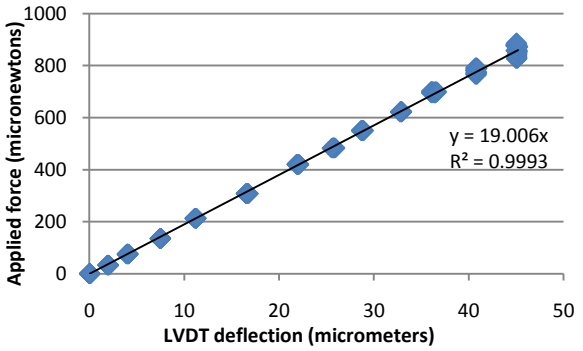

Figure 8: Typical Calibration Result, December 8th 2009

This is not formally 'correct', since the independent variable is actually the deflection on the LVDT- experimenters are controlling the applied force. Still, when plotted in this way the slope of the data is directly the "sensitivity" of the thrust stand in the convenient units of N/m (or micronewtons/micrometer). This

number can then be directly multiplied by the deflection of the thrust stand when any actual thruster is turned on to get the thrust developed by the thruster- this greatly simplifies data reduction. As a note, if the data seems particularly unreliable on a given day- much oscillation, a mysteriously large hysteresis, or if the thrust stand configuration has been changed recently- multiple runs are taken to ensure that the sensitivity being measured is accurate.

Many factors affect the sensitivity of the torsional thrust stand. It is not even entirely certain that all of them are known- the ones that are not known, however, are part of the 'noise' that causes results to vary slightly from day to day, which is the reason why all experimental days start with a fresh calibration run as above performed in high vacuum to ensure acceptably accurate results. Two groups of factors have been observed to most affect sensitivity. The first are things that directly increase or decrease the rotational inertia of the thrust stand, such as adding mass or connecting additional wires with a finite stiffness to the rotating part of the thrust stand. The second group is RF cable heating. Again, many other effects which would be expected to affect sensitivity such as pressure in the vacuum chamber are lost in the statistical noise.

Although intuitively, adding wires or mass to the thrust stand should decrease sensitivity and can be compensated for by minimizing connections and mass, wire heating is a problem that has not yet been solved and very likely has no ideal solution. Metals expand when heated. Because of this, even with insulation coaxial cables will expand when heated. Because no cable is perfect, a fraction of the RF power being streamed through a cable will dissipate into heat, causing the cable to warm up and expand. None of these facts can be changed, as unfortunate as they are- linear expansion of the RF cables, with a small but nonzero percentage being out of the thrust stand plane of rotation acts like a 'phantom' thrust and places a torque on the thrust stand which shows up as a deflection on the LVDT. A significant amount of effort went into draping the cables to cause minimum distortion of the results; while ameliorating the effect, still could not solve the problem. A significant amount of time was invested in characterizing this expansion. It was found that when power was placed on the RF cable, the resulting heating and expansion could cause the deflection on the thrust stand to continue for up to one hour with a severity of up to 30-40 micrometers; while not sounding severe, this is larger than the expected deflection from thruster operation in most of the design space. The problem was solved by noting that after ~5-10 minutes, the LVDT deflection increased almost perfectly linearly with a rate of less than 1 micrometer per minute. This small a drift, when so close to linear, can be mathematically reduced out of the raw data.

The final aspect of calibration relevant to this paper is testing sensitivity, so that it can be said with confidence that the thrust stand is measuring a force plus or minus some number of micronewtons. To test this, entire runs were performed doing the following. Taking the thrust stand to a given thrust level, for example 90 micronewtons, the voltage was adjusted by exceptionally small amounts- 1 or 2 volts, corresponding generally to the same number of micronewtons. Data was taken for a range of 10 or so volts, as well as returning to the starting point to check for hysteresis, just as though it were a normal calibration run. A sample result is shown in Figure 9 below. The limiting factor for accuracy of our thrust stand is the shaking of the LVDT by approximately +/- 100 nanometers. This approaches the point where random electrical noise interferes with the LVDT signal, as well as the limits of the LVDT's designed resolution itself. 100 nanometers, after all, is smaller than most *bacteria*. This horizontal smearing translates to a loss of accuracy in measuring force- below, with the line drawn to encompass most of the data points, it has a 'height' of 1.5 micronewtons. Because of this result, and its repeatability, we can say with high confidence that when we measure a force around 90 micronewtons it is what we measure plus or minus just under 1 micronewton. Similar tests were run at a number of thrust levels, with similar results. Because of these calibrations, a general guideline of +/- 1-2 micronewtons has been shown to be a reasonable error value throughout the plausible performance range of the RF microthermal thruster on the LEAP torsional thrust stand.

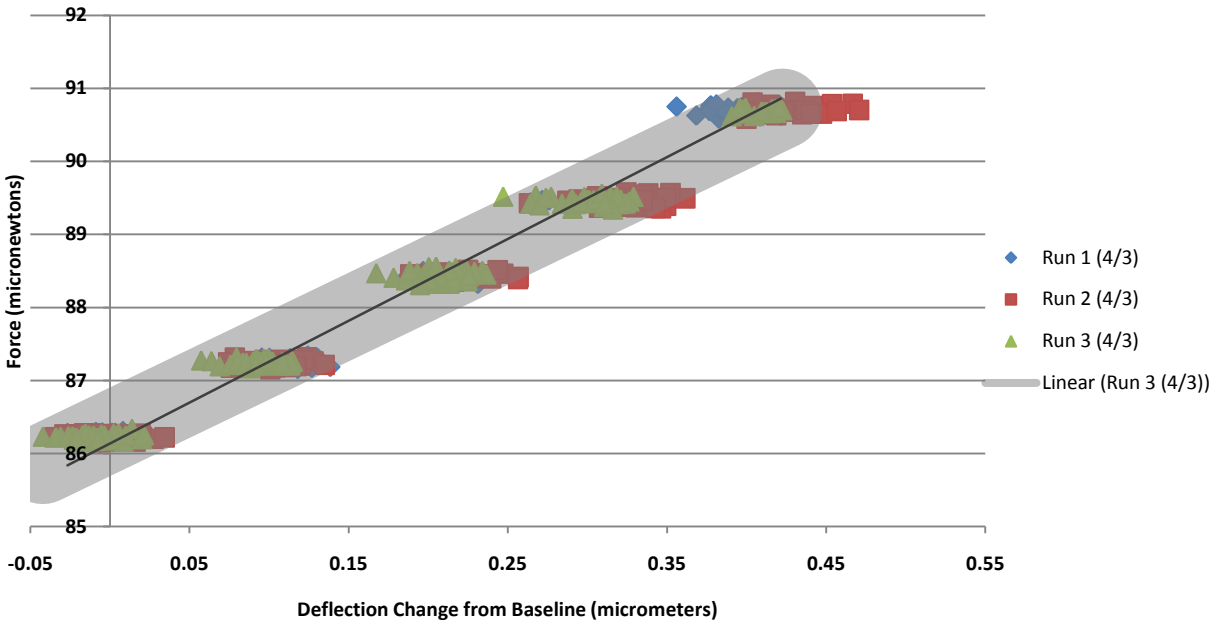

Figure 9: Sensitivity Test at the 90 Micronewton Regime

Testing Results

Preliminary results have focused on sampling a small but representative area of the final planned design space. Two different thruster configurations would be examined, one with no nozzle plate and one converging nozzle with a 0.025" throat diameter made of clear plastic. Plastic was chosen for this preliminary set of runs so conditions inside the thruster could be seen and plasma formation visually verified. The first test on any given day was a cold gas test, where room temperature argon was streamed through the thruster configuration being studied to have the best possible baseline for the day's tests.

The same basic procedures were followed for cold gas and 'hot' gas tests with RF power on. Mass flow was increased to ~1.1 mg/s and then decreased back to 0 by varying steps to check for hysteresis. While results for cold gas were extremely linear and uniform, the specific impulse was ~20% lower than theoretical for argon exhausting at sonic velocity due to various losses. These losses should not change much for hot gas tests, and should be able to be eliminated in a production thruster. For this reason, the primary figure of merit in later graphs is 'improvement over cold gas' instead of a direct specific impulse or thrust.

To get a broad overview of how the thruster operates, for each nozzle configuration a pair of test series were run. One would keep the frequency constant at 140 MHz- an arbitrarily picked frequency in the middle of the range under study- and vary RF power supplied as well as mass flow rate through the thruster. The other would keep the power constant at 40 W (not counting impedance mismatch losses, which were ~40% of supplied power) while varying frequency and mass flow rate. These tests revealed interesting results. The first test series, a "power sweep" for the 0.025" plastic nozzle, is shown below in Figure 10 with error bars on the thrust measurement of plus or minus a standard deviation- these will not be placed on graphs in the remainder of this paper, as with the volume of data it clutters graphs and does not markedly change in magnitude with different test series.

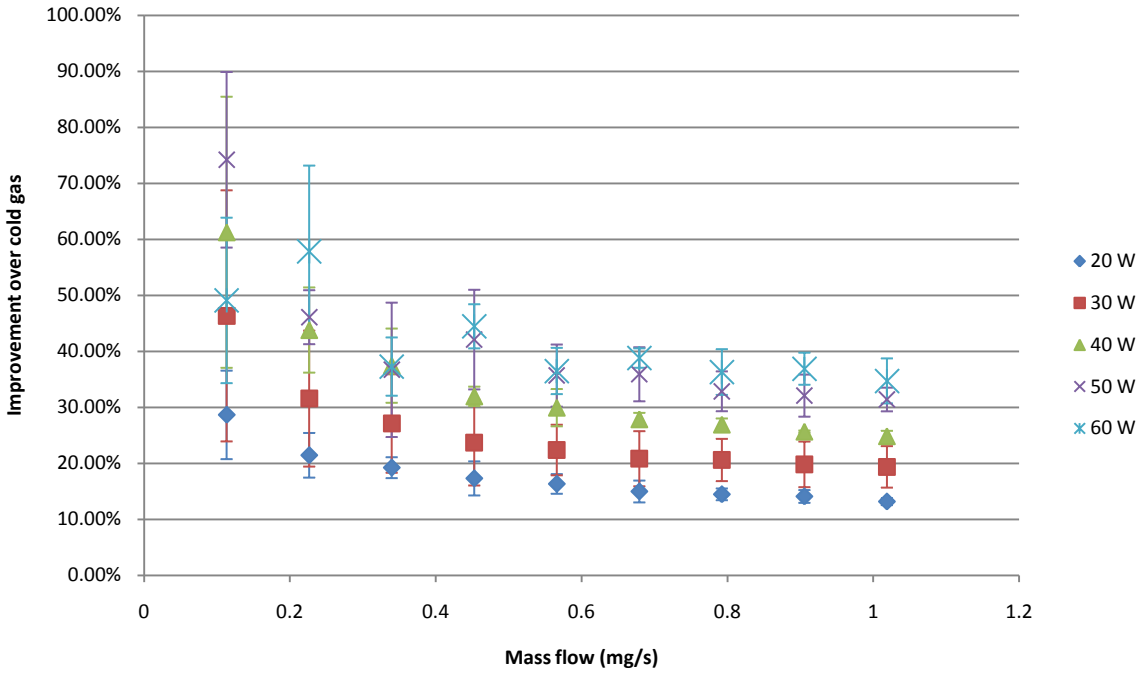

Figure 10: Power Sweep Results, Plastic 0.025" Nozzle, 140 MHz frequency

The most important result from this graph is that, in accordance with theory, a trend with mass flow rate is visible- at high mass flow rates of greater than ~0.3 mg/s, the improvement in thrust over cold gas at the same mass flow rate and configuration is a near constant. As mass flow rate decreases below that, however, the comparative advantage of powered thrust jumps significantly. This is a sign that there is a heating effect going on which is nonlinear with mass flow- a certain amount of heating occurs 'no matter what', with additional heating past that linear with mass flow. The mechanism for this behavior is available from even the simplified model presented earlier. Stochastic heating delivers a relatively constant amount of heat to the flow in watts regardless of mass flow rate, but ohmic heating depends strongly on pressure in the thruster and hence mass flow rate. Because of this, as pressure and mass flow rate drop, the power delivered to the flow does not commensurately drop and the heating is greater. Furthermore, also in accordance with theory, Figure 10 shows that with a few errors that are probably random noise the thrust derived scales linearly with power. To show this more clearly, a single mass flow rate was taken from Figure 10 and graphed on its own; Figure 11 shows the thrust vs. power behavior at a single mass flow rate and frequency, which confirms the intuitive and theory-supported hypothesis that heating and thrust scale linearly with power.

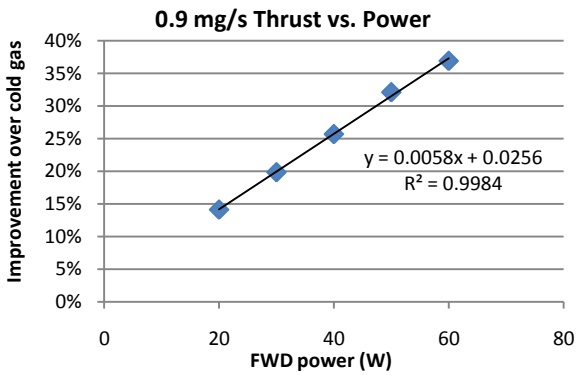

Figure 11: Linearity of Thrust with Increasing Power

The frequency sweep, shown below in Figure 12, has another striking behavior- a strange variation in behavior with applied frequency and mass flow rate. For most of the frequencies studied, the familiar upward trend effect as massflow approaches zero shows up clearly. For a few frequencies, however, performance remains flat. What this reveals is that, if the two-heating-mechanism hypothesis above is correct, then **stochastic heating does not increase with frequency as the simplified model suggests.** Rather, it behaves unpredictably, probably due to the copious assumptions made- as an aside, however, Ref. 6 and the more rigorous particle-in-cell analysis of the RF microthermal thruster also do not show anything

approaching this behavior. Because of this nonlinear interaction of frequency and mass flow rate, and because the interaction is so strong- 80% thrust improvement versus 20% thrust improvement at the same mass flow rate and input power corresponds to a difference of hundreds of degrees Kelvin- this forms the justification for further study to find out exactly how much thrust can be gleaned from this thruster. This will be further explored in future work.

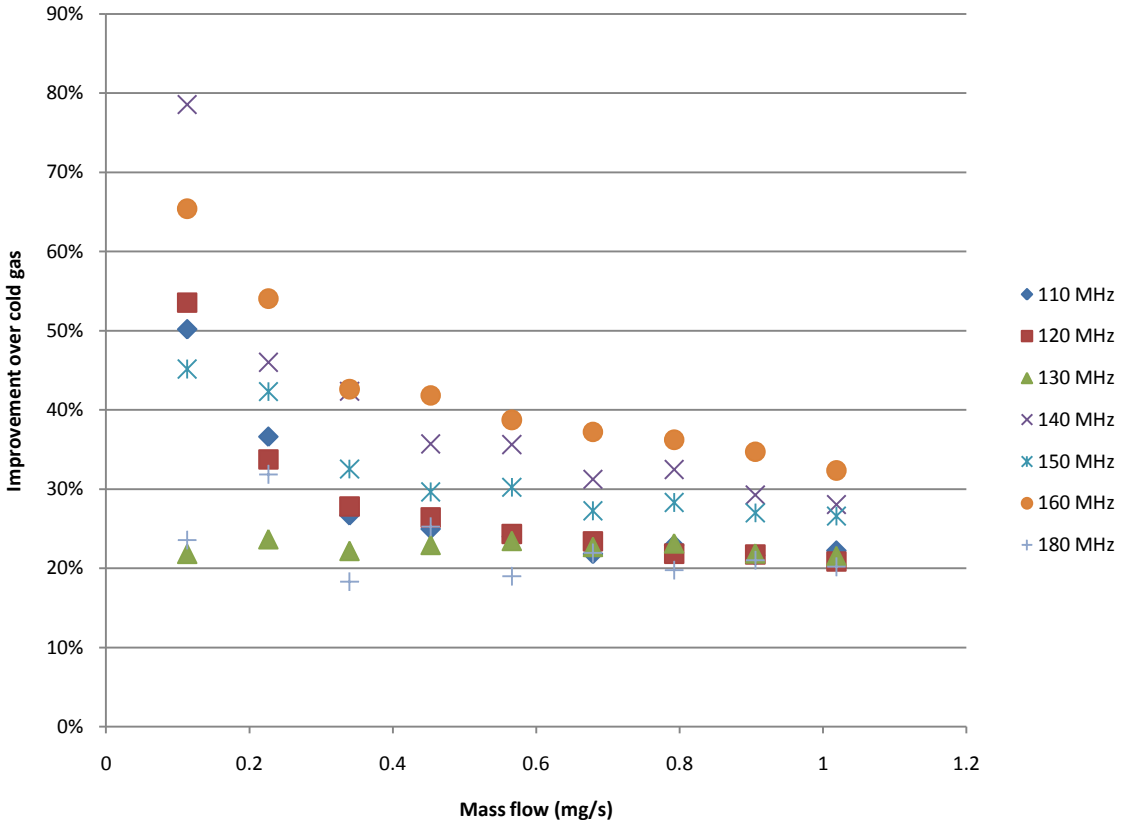

Figure 12: Frequency Sweep Results, 40 W power, Plastic 0.025" Nozzle

The next step in testing was to repeat the above without any nozzle plate on, so that the thruster chamber was open to the vacuum chamber. In effect, this made the 'nozzle diameter' ¾" instead of 0.025". This in turn drastically increased velocity inside the thruster and dropped residence time, which logically would give massive drops in heating and thrust. In addition to this, the results of the power sweep shown in Figure 13 were very chaotic. It does not at first glance show any reasonable trend aside from the familiar leap upwards at 0.1 mg/s. An important observation is the *size* of the improvement over cold gas, which is around 1/3 to ½ of the improvement seen with the nozzle on, which makes intuitive sense. The cold gas thrust for both nozzle-on and nozzle-off cases were within a few percent of each other, which also makes intuitive sense because an equal mass flow rate of the same gas is being piped through both and exiting through a choked orifice- the only difference is the different pressures inside the thruster, and the slight cold gas thrust difference is accounted for by that pressure thrust.

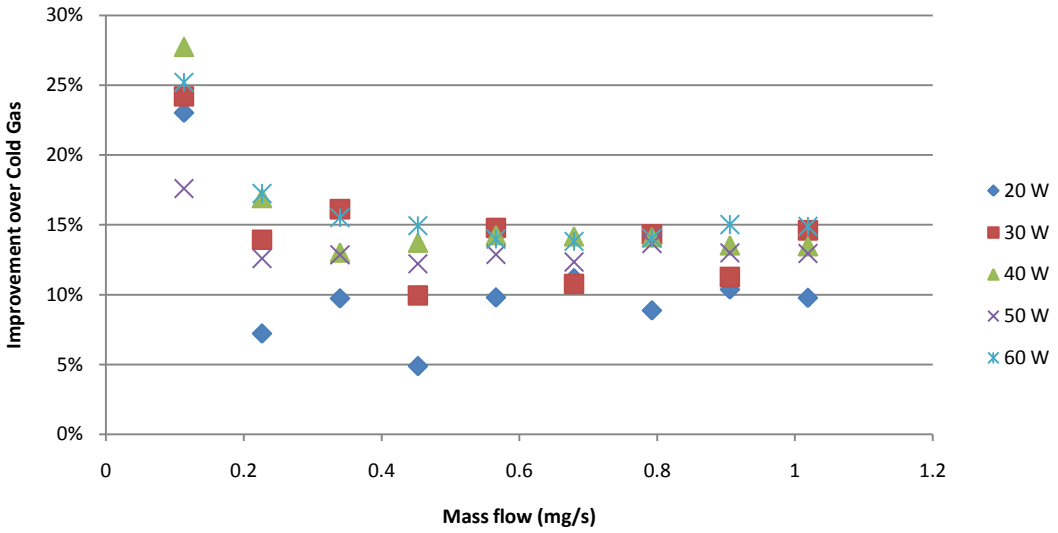

Figure 13: Power Sweep Results with No Nozzle

Although chaotic, when individually graphed there is a slight upward trend to the thrust derived versus power input. The other important observational result from this series of tests was that the thruster did not 'light' without a nozzle plate on- that is, no visible excitation of the argon occurred, indicating much less ionization. The frequency sweep with no nozzle yielded more intriguing results, especially when combined with the frequency sweep with nozzle on. Figure 14 shows the nozzle on frequency sweep data plotted in a different way, and Figure 15 shows an equivalently formatted plot of the frequency sweep data without a nozzle. Both show an increase at low mass flow rates of thrust, and both still show a nonlinear variation in thrust with frequency, and as previously mentioned the magnitude of thrust improvement is approximately cut to a third when the nozzle is removed. What is more interesting is that that variation is identical at a constant configuration with varying mass flow rate. Most interesting of all, however, is that the qualitative character of that variation changes between geometries. These changes indicate that there is a complex and ill-understood interplay between thruster geometry, applied frequency, and mass flow rate that have an extremely large effect on important performance parameters that merits further study.

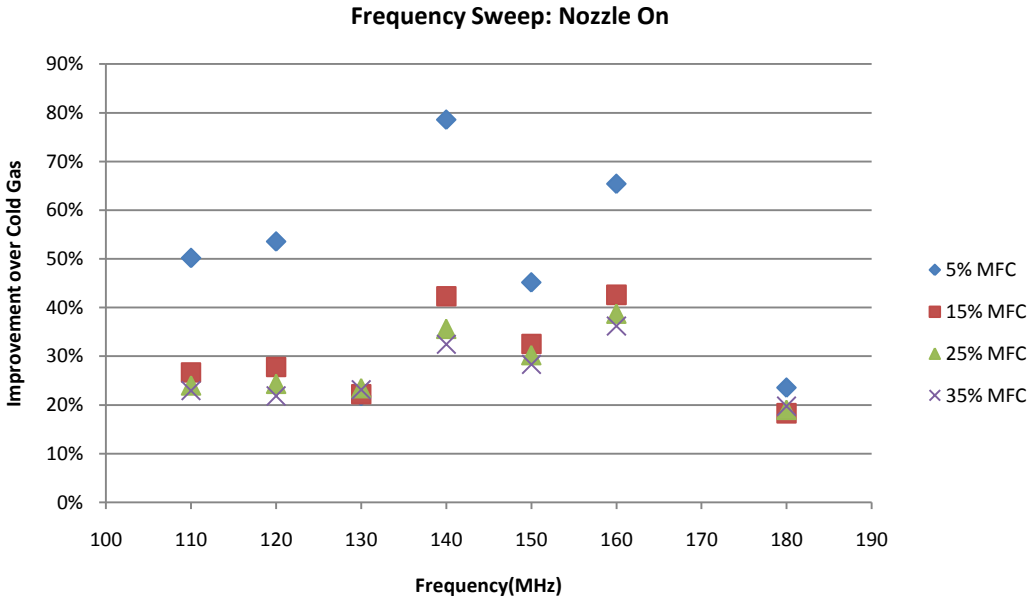

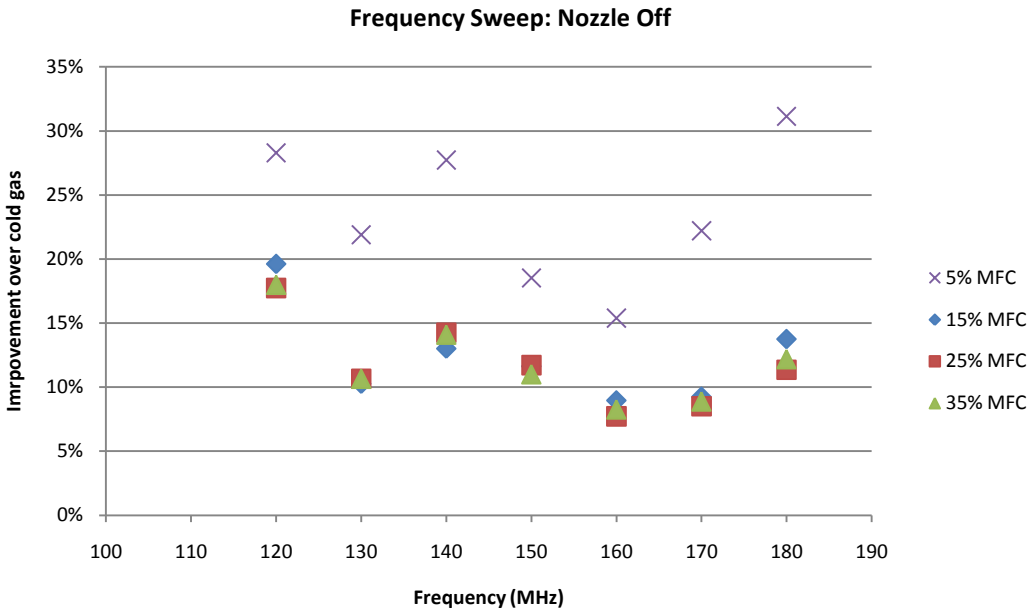

Figures 14 and 15: Frequency Sweeps at Different Configurations

With the tests performed so far, few certain conclusions can be drawn past the one reached earlier that thrust scales approximately linearly with power. What can be confidently said is to restate the above, that mass flow rate, RF power frequency, and thruster geometry interact in complex and nontrivial ways to produce wildly different amounts of heating inside the thruster, which translates to additional thrust greater than would be achieved by simply streaming argon without heating. Without optimization of the thruster or frequency, the highest specific impulse so far is an increase of 80% over cold gas, or approximately 81-82 seconds of Isp. This nontrivial and large variation of thrust in addition to the gain just from altering the power justifies much further work towards both understanding these phenomena and making use of them to create a new, more efficient propulsive device.

Finally, the experimental results were compared with the theoretical model constructed above, with the results shown in Figure 16. The solid lines are what theory would predict for a given run, while the points are what actually was measured. There is a good agreement in trend, both with mass flow rate and with power. Where there is not a good agreement is in magnitude, especially at lower mass flow rates. The higher mass flow rate becomes, the closer theoretical and experimental results cleave to each other. This would indicate that the heating mechanism dominant at mass flow rates, stochastic heating, is at fault. Furthermore, that was the heating mechanism blamed above for the strange behavior of thrust with frequency. Combining those results and the difference between theoretical and actual results, it is clear that stochastic heating does not behave the way the theory says it should behave. This opens up future avenues of exploration, because- as can be seen in the figure below- if stochastic heating can be brought more in line with theoretical prediction through better understanding the relevant inefficiencies arising from geometry, massive performance improvements could result.

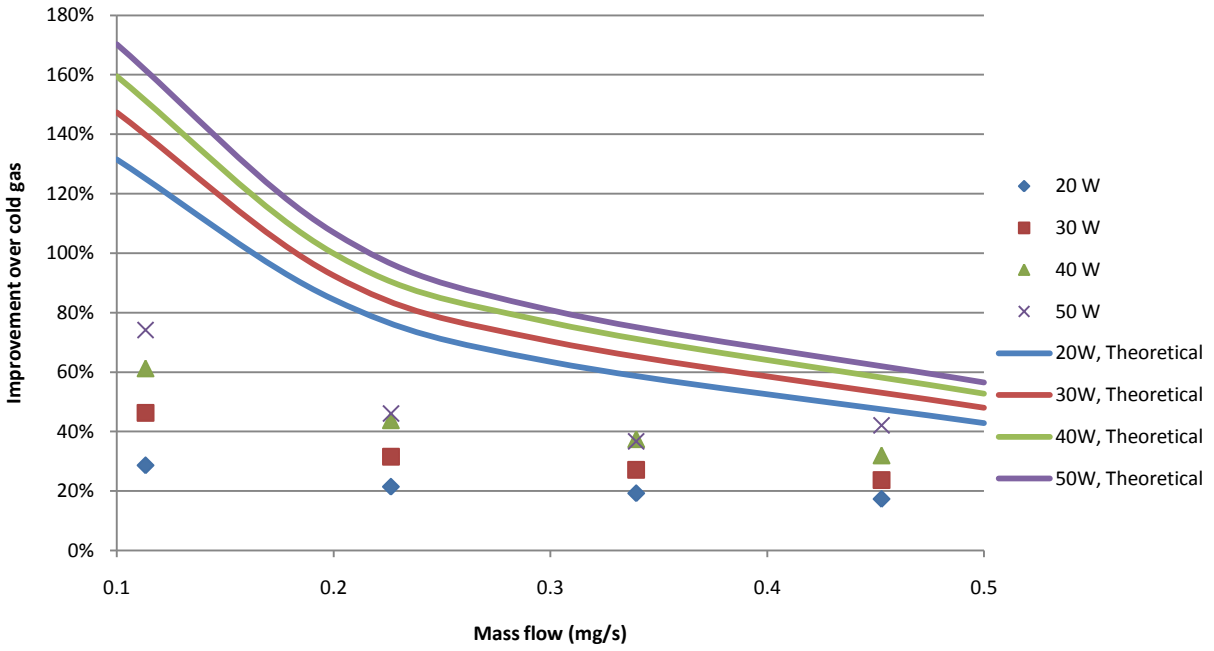

Figure 16: Theoretical vs. Experimental Results at 140 MHz with Nozzle On.

FUTURE WORK

Since the most important and experimentally 'interesting' effect on performance is in the interplay of frequency, mass flow rate, and thruster geometry, follow-up research will focus mainly on those topics. Frequency sweeps will be performed at different power levels to verify that the same behavior shows up at multiple power levels. Thruster geometry will be changed, and frequency sweeps performed with the different geometries. Nozzle throat/orifice size will be a major experimental variable, to examine whether the thrust changes linearly with that diameter as a basic theoretical assumption would indicate due to linearly increasing thruster chamber pressure. In addition, aluminum nozzle plates instead of plastic will be tested to check if the different electrical field structure inside the thruster with a conductor at the end instead of an insulator can increase thrust. Electrode diameters and lengths are also planned to be examined. Finally, at least one gas other than argon will be tested as a propellant- lighter noble gases such as neon should work well and deliver higher performance if the heating characteristics are similar. Diatomic gases such as nitrogen are not anticipated for study, however, as aluminum nitride deposits on the dielectric and electrodes have been shown to limit thruster lifetime.

Once this work has been concluded, the lessons drawn from the data will go into the design and machining of a second-generation thruster prototype designed to emphasize the positive effects on performance as much as feasible with LEAP's limited facilities and to be a stepping stone towards a potential future production thruster. With the limited testing so far, thrust improvements of 80% over cold gas (corresponding roughly to 80 seconds Isp, with argon) have already been demonstrated. It seems reasonable that further tweaking of parameters with this thruster body can improve that value to 100 seconds or greater, with an ultimate goal of tripling performance over cold gas. The limiting factor is heat transfer to the thruster body- above some value of plasma temperature, equilibrium will be reached with convective heat transfer into the thruster even at the low densities anticipated, balancing the electromagnetic heat transfer into the fluid.

CONCLUSION

A need for microsatellite propulsion systems in the 10-100 micronewton range has been found, and the RF microthermal thruster is a promising candidate to fill that niche. A simplified analytical model has been presented, and predictions for performance that indicate possible specific impulses high enough to justify investigation shown to result from that model. The procedures, calibrations, and results of early experimental testing have been presented, which show that thrust improvements of the qualitative type predicted do occur in a laboratory environment, but that due to unforeseen inefficiencies in design the amount of performance increase is not yet sufficient. A comparison of theoretical and experimental results, combined with the nonlinear and erratic trends seen in

other experimental results, indicate that via intelligent design of the thruster and a more rigorous examination of the design space the theoretical results can be more closely approached. If true, the RF microthermal thruster will become a competitive low-thrust microsatellite thruster.

ACKNOWLEDGMENTS

The authors would like to thank Purdue University for their financial support for the duration of the research. Additionally, Patrick Huu provided valuable day to day support in the laboratory.

REFERENCES

1. Gurtuna, O. "Emerging Space Markets: Engines of Growth for Future Space Activities" Recent Advances in Space Technologies, 2003. RAST '03. 20-22 Nov. 2003 pp.536 - 541
2. Surrey Satellite Technology Limited data sheet. Retrieved from http://www.sstl.co.uk/assets/Downloads/Gas%20Propulsion%20System.pdf 12/15/09.
3. Scharlemann and Tajman, Development of Propulsion Means for Microsatellites, 43rd AIAA/ASME/SAE/ASEE Joint Propulsion Conference and Exhibit, Cincinnati, OH, July 8-11, 2007; AIAA-2007-5184.
4. Ziemer, Laser Ablation Microthruster Technology. 33rd Plasmadynamics and Lasers Conference, Maui, Hawaii, May 20-23, 2002; AIAA-2002-2153.
5. R.A. Spores, G.G. Spanjers, M. Birkan, and T.J. Lawrence. Overview of the USAF Electric Propulsion Program. 37th Joint Propulsion Conference, Salt Lake City, Utah, July 8-11 2001. AIAA 2001-3225.
6. Stein, Alexeenko and Hrbud. Performance Modeling of a Coaxial Radio-Frequency Gas-Discharge Microthruster. Journal of Propulsion and Power, Vol. 24, No. 5, September–October 2008; AIAA 34036-184.
7. Chianese and Micci, Microwave Electrothermal Thruster Chamber Temperature Measurements and Performance Calculations. JOURNAL OF PROPULSION AND POWER Vol. 22, No. 1, January–February 2006; AIAA-15337-269.
8. Mistoco and Bilen, Numerical Modeling of a Miniature Radio-Frequency Ion Thruster, 44th AIAA/ASME/SAE/ASEE Joint Propulsion Conference & Exhibit 21 - 23 July 2008, Hartford, CT; AIAA-2008-5194-922.
9. Allan Yan, Bradley Appel, and Jacob Gedrimas. Millinewton Thrust Stand Calibration Using Electrostatic Fins. 47th AIAA Aerospace Sciences Meeting, 5 - 8 January 2009, Orlando, Florida; AIAA-2009-212-184.